


8-7-2019

Subsurface MIMO: A Beamforming Design in Internet of Underground Things for Digital Agriculture Applications

Abdul Salam

Purdue University, salama@purdue.edu

Follow this and additional works at: https://docs.lib.purdue.edu/cit_articles

 Part of the [Agricultural Economics Commons](#), [Digital Communications and Networking Commons](#), [Sustainability Commons](#), and the [Systems and Communications Commons](#)

Salam, Abdul, "Subsurface MIMO: A Beamforming Design in Internet of Underground Things for Digital Agriculture Applications" (2019). *Faculty Publications*. Paper 21.

https://docs.lib.purdue.edu/cit_articles/21

This document has been made available through Purdue e-Pubs, a service of the Purdue University Libraries. Please contact epubs@purdue.edu for additional information.

Article

Subsurface MIMO: A Beamforming Design in Internet of Underground Things for Digital Agriculture Applications

Abdul Salam ^{1,*}

¹ Department of Computer and Information Technology, Purdue University, West Lafayette, IN 47907, USA; salama@purdue.edu

* Correspondence: salama@purdue.edu; Tel.: +1-765-496-6867

† This paper is an extended version of our paper published in International Conference on Internet of Things (ICIOT 2019), San Diego, CA, USA, June 2019 [1].

Version August 10, 2019 submitted to J. Sens. Actuator Netw.

Abstract: In underground (UG) multiple-input and multiple-output (MIMO), the transmit beamforming is used to focus energy in the desired direction. There are three different paths in the underground soil medium through which the waves propagate to reach at the receiver. When the UG receiver receives a desired data stream only from the desired path, then the UG MIMO channel becomes three path (lateral, direct, and reflected) interference channel. Accordingly, the capacity region of the UG MIMO three path interference channel and degrees of freedom (multiplexing gain of this MIMO channel requires careful modeling). Therefore, expressions are required for the degree of freedom of the UG MIMO interference channel. The underground receiver needs to perfectly cancel the interference from the three different components of the EM-waves propagating in the soil medium. This concept is based upon reducing the interference of the undesired components to a minimum level at UG receiver using the receive beamforming. In this paper, underground environment aware MIMO using transmit and receive beamforming has been developed. The optimal transmit beamforming and receive combining vectors under minimal inter-component interference constraint are derived. It is shown that UG MIMO performs best when all three component of the wireless UG channel are leveraged for beamforming. The environment aware UG MIMO technique leads to three-fold performance improvements and paves the way for design and development of next generation sensor-guided irrigation systems in the field of digital agriculture. Based on the analysis of underground radio wave propagation in subsurface radio channel, a phased array antenna design is presented that uses water content information and beam steering mechanisms to improve efficiency and communication range of wireless underground communications. It is shown the subsurface beamforming using phased array antenna improves the wireless underground communications by using the array element optimization and soil-air interface refraction adjustment schemes. This design is useful for subsurface communication system where sophisticated sensors and software systems are used as data collection tools that measure, record, and manage spatial and temporal data in the field of digital agriculture.

Keywords: Digital Agriculture; Wireless Underground Channel; Underground Communications; MIMO; Beamforming; Internet of Underground Things

1. Introduction

The purpose of digital agriculture is to tailor agricultural inputs and processes to localized environment in the farm to apply correct practices in the field in a timely and correct manner. It leads to development of smart and digital sensing, communications, and real-time decision making systems

32 to sense, analyze, detect, and manage the soil and farm specific spatial and temporal patterns in the
33 field for sustainability, profitability and to protect the environment [2], [3], [4].

34 Internet of Underground Things (IOUT) have many applications in precision agriculture [5], [6],
35 [7], [8], [9], [10], [11], [12], [2], [3], [4], [13], [14], [15], [16], [17], [18], [19], [1], [20], [21], [22], [23]. Border
36 monitoring is another important application area of IOUT, where these networks are being used to
37 enforce border and stop infiltration [24], [25]. Monitoring applications of IOUT include land slide
38 monitoring, and pipeline monitoring [9], [26], [27], [28]. IOUT provides seamless access of information
39 collected from agricultural fields through the Internet. IOUT include in situ soil sensing capabilities
40 (e.g., soil moisture, temperature, salinity), and provide the ability to communicate through plants and
41 soil, and real-time information about the environment (e.g., wind, rain, solar). When interconnected
42 with existing machinery on the field (seeders, irrigation systems, combines), IOUT enable complete
43 autonomy on the field, and pave the way for more efficient food production solutions. At agricultural
44 farm level, IOUTs are being used to provide valuable information to the farmers.

45 By using software defined control of individual antenna elements, steering solutions for
46 communications with static and mobile above-ground devices in digital agriculture can be
47 implemented [1,29]. This kind of implementation of underground (UG) beamforming is challenging
48 due to many reasons. The major challenge is the phase shift between antenna elements. To get a desired
49 beam pattern, the phase shifts between antenna elements need to be equal in the desired direction. This
50 requires calibration of phase shifters and dynamic on-the-fly phase correction to achieve the desired
51 beam. To address these challenges, digital beamforming using phased array antennas based on soil
52 moisture conditions to form dynamic beam patterns can be employed. We have investigated three
53 different array designs. First design consists of two separate linear arrays each with its own phase
54 shifter with pre-defined parameters for communication with underground and aboveground arrays.
55 Furthermore, beams are stitched such that a number of beam patterns are determined and designed
56 based on the analyses of underground and above-ground devices and stored in configuration database
57 for on-demand usage. The second design is based two arrays stacked at different UG depths with
58 phase shifting done in the software. This approach is based on processing in the software defined radio
59 to adapt to wavelength changes due to soil moisture conditions. The advantage of using this approach
60 is that dynamic changes in the wavelength and phase variations due to UG channel dynamism can
61 be compensated without changing physical array arrangements. Moreover, less energy is required in
62 comparison to traditional mechanical phase shifters. In the third design, the multi-dimensional arrays
63 structure such as rectangular, planar, and circular arrangements to to have simultaneous beams in
64 multiple planes are used.

65 UG transmit beamforming using phased array antennas at the transmitter [29] has been used in
66 the underground (UG) communications to maximize the lateral wave [30] by transmitting energy at a
67 particular angle. By using this approach, the energy wastage by sending signals in isotropic direction
68 is reduced by forming the narrow-width beam and steering it accordingly. In underground wireless
69 communications, the aim is to enhance the received signal strength and reduce the interference at
70 the receiver. In over the air (OTA) wireless communications, a strong signal strength is attained by
71 transmitting the signal from multiple antennas by different amplitudes and phases. Through this
72 approach, the received signal components add coherently at the receiver. However, in underground
73 communication due to different wave propagation speed in different communication mediums (e.g.,
74 soil and air), coherent combining at the receiver in a constructive manner can not be achieved.
75 Therefore, an environment aware UG multiple-input and multiple-output (MIMO) design is required.

76 The line-of-sight (LoS) component between the UG transmitter and receiver has limitations
77 because of the higher attenuation in the soil medium. An example power delay profile (PDP) of
78 wireless UG channel is shown in Fig. 1. Moreover, the direct path has shorter range and can not be
79 used to reach at longer distances in the underground medium. Therefore, combined transmit and
80 receive beamforming needs developed using non-LoS components (e.g., lateral and reflected). Since,
81 multipath underground channel well-known [30] and has been studied and empirically validated, UG

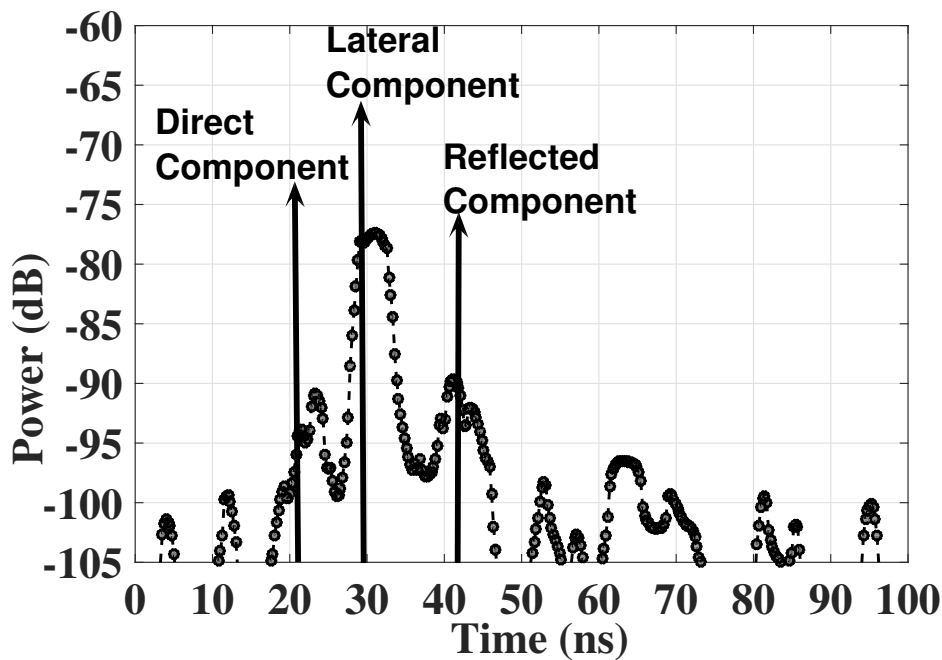


Figure 1. An example power delay profile (PDP) of the impulse response model of the wireless UG channel [30].

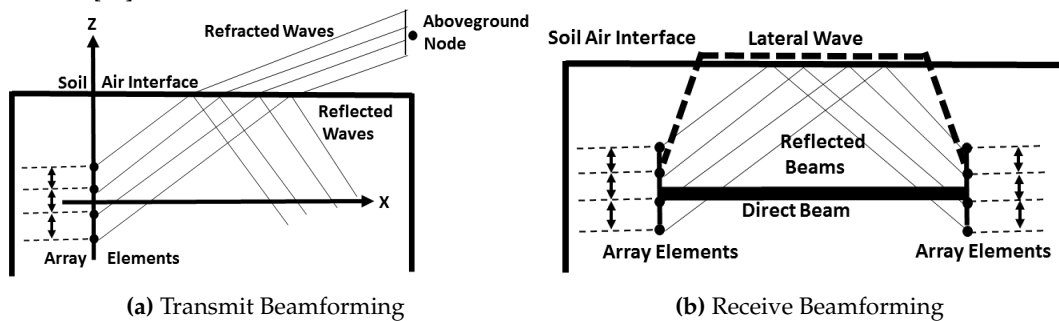


Figure 2. The communications schematic for UG MIMO.

82 MIMO can be developed for high data rate and log range communications. In this work, techniques
 83 have been developed to maximize the signal strength and minimizing the interference at the receiver.
 84 Moreover, UG MIMO beamforming expressions have been developed to maximize the capacity of the
 85 underground communications.

86 The rest of the paper is organized as follows: the background and major contributions of this
 87 work are discussed in Section 3. The UG MIMO is modeled in Section 4. Performance evaluations are
 88 done in Section 5. The article concludes in Section 7.

89 2. Related Work

90 An empirical analyses using off-the-shelf sensor motes to characterize the path loss in UG channel
 91 has been conducted in [30], and accordingly path loss models for underground-to-underground
 92 (UG2UG) and underground-to-aboveground (UG2AG) channels have been developed in [19,20].

93 Moreover, digital agriculture solutions including enabling technologies [14], subsurface antenna
 94 design [17,18], underground cognitive radio [31], and soil moisture sensing using subsurface radio
 95 wave propagation [15] have been developed for Internet of Underground Things [22,23]. Accordingly,
 96 we devised an subsurface planar antenna [17,18], which combats adverse effects of time-variant
 97 subsurface radio channel characteristics and extends communication ranges of underground radios.

98 This allows for development of architectures for connected soil moisture sensing networks and
99 automated irrigation solutions [23], [22]. Moreover, it is shown that software defined operation in
100 underground communications can extend the capacity of UG channel [12,32]. The development of IoT
101 based smart security and monitoring devices for agriculture has been investigated in [33]. A survey on
102 advances in magnetic induction-based wireless underground sensor networks has been presented in
103 [34]. A secure smart agriculture monitoring technique through isolation is developed in [35]. The IoT
104 vision, key features, applications, and open issues are discussed in [36]. IoT in agriculture, its recent
105 advances, and future challenges are outlined in [37].

106 Beamforming antennas [38] are being used in wireless networks to reduce interference and
107 improve capacity. Beamforming have been addressed in [39], [40], [41], [42], [43], [44], [45], [46], [47]
108 for over-the-air (OTA) wireless channels and in [48] for MI power transfer, but no existing work has
109 considered the underground beamforming. In UG communications, lateral component [49] has the
110 potential, via beam-forming techniques, to reach at farther UG distances which otherwise are limited
111 (10 m to 15 m) because of higher attenuation in soil [30].

112 3. Contributions of This Work

113 This is the first work to design a fully UG MIMO for the UG communications. The transmit and
114 receive beamforming techniques are considered which communicate through the soil by using UG
115 channel medium. Based on the receiver position, EM waves either travel completely through soil for
116 UG communications or some part of it goes through the air for aboveground(AG) communications.

117 We leverage an UG channel impulse response model for UG beamforming perspective and
118 identify the major EM wave components. Challenges in UG beamforming are highlighted and use of
119 of UG MIMO is motivated. We present the effects of different soil properties on beamforming vectors
120 of the transmitter and receiver. This proposed mechanism estimates the best beam steering angle based
121 on the soil moisture sensing.

122 We have considered an UG MIMO transceiver system where both transmitter and receiver has
123 the beamforming capability. Additionally, this approach removes the inter-component interference
124 and enhance the received signal strength. Underground environment aware MIMO using transmit
125 and receive beamforming is vital to increased spectral efficiency, enhance communication range, and
126 energy efficiency in next-generation wireless underground networks, which are expected to include
127 underground antenna arrays [29]. UG MIMO approach has potential applications in many practical
128 scenarios such as precision agriculture, ground penetrating radars (GPR), hazardous object search,
129 locating IEDs, transmission structures under the runways for aircraft communications, antennas
130 for geographic research, communications from marshes, geology, and wireless underground sensor
131 networks (WUSNs).

132 4. The UG MIMO System Models

133 The underground nodes communicate with other underground nodes (UG2UG link) and above
134 ground nodes (UG2AG link). Communications schematic for UG MIMO communications is shown
135 in Figs. 2. These aboveground nodes are fixed sinks and mobile nodes mounted on movable
136 infrastructures such as center pivot. In aboveground communications, waves propagating to receiver
137 nodes are refracted from soil-air interface, whereas in UG communications, lateral waves need to be
138 utilized. Desired beam patterns for both scenarios are shown in Figs. 2. In Fig. 2(a), that refractions
139 and reflections of EM waves from the soil-air interface effect the beam patterns propagating to the
140 above-ground node.

141 In UG MIMO, transmit beamforming [29] is used to focus energy in the desired direction, there
142 are three different paths [30] in the underground soil medium through which the waves propagates to
143 reach at the receiver. When the UG receiver receives a desired data stream only from the desired path,
144 then the UG MIMO channel becomes three path (lateral, direct, and reflected) interference channel.
145 Accordingly, the capacity region of the UG MIMO three path interference channel and degrees of

146 freedom (multiplexing gain of this MIMO channel requires careful modeling. Therefore, expressions
147 are required derived the degrees of freedom of the UG MIMO interference channel.

148 The underground receiver needs to perfectly cancel the interference from the three different
149 components of the EM-waves propagating in the soil medium. in UG transmit beamforming, limited
150 number of antenna can only achieve low spatial directivity, that leads to presence of signals in undesired
151 direction that cause interference at the receiver. This UG MIMO concept is based upon reducing the
152 interference the undesired components to minimum at UG receiver using the receive beamforming.
153 In this paper, underground environment aware MIMO using transmit and receive beamforming has
154 been developed. The optimal transmit beamforming and receive combining vectors under minimal
155 inter-component interference constraint are derived. Accordingly, UG MIMO techniques are designed
156 and investigated in the underground soil medium. Next we present the system model:

157 We consider an UG MIMO transceiver system where both transmitter and receiver has the
158 beamforming capability. We also consider that the transmitter node is equipped with two or more
159 transmit antennas and has the beam steering capacity. The receiver node is also equipped with
160 multiple antennas and can receive all three components propagating through underground medium.
161 In this paper, we also assume that the UG MIMO receiver has path selection and switching capability
162 through a selection mechanism which is based on the strength of the received paths at the receiver.
163 Throughout the development of this approach, we also assume equal power allocation at the UG
164 MIMO transmitter. To analyze the achievable capacity using environment aware MIMO using transmit
165 and receive beamforming, we also assume a total power constraint.

166 Next, we present a zero forcing (ZF) UG MIMO transceiver technique. This approach does not
167 requires the availability of the channel state at the receiver in contrast to the OTA MIMO techniques.
168 Additionally, this approach removes the inter-component interference and enhance the received
169 signal strength. The channel between the underground transmitter T and underground receiver R is
170 represented by \mathbf{TR} of size $N_t \times N_r$ with complex values, where N_t and N_r represents the number of
171 transmit and receive antennas, respectively. The k spatial underground components are distinguished
172 using the w_1, \dots, w_k where w is associated with component. A $N_t \times N_r$ matrix \mathbf{I}_k denotes the
173 interference between different components. The received signal at the underground receiver by using
174 equal power constraint is given by [50]:

$$y_k = \mathbf{w}_k^* \mathbf{TR} \mathbf{f}_k x_k + \mathbf{w}_k^* \mathbf{I}_k \mathbf{f}_i x_i + \mathbf{w}_k^* n_k \quad (1)$$

175 where x_k is the transmitted signal of the UG component k , and w_k and f_k are the transmit and
176 receive beamforming vectors, n_k is additive white Gaussian noise (AWGN) vector.

177 Next, we present the expression to maximize the capacity for the low SNR case. From the (1), the
178 received SINR at the UG receiver at the k th component can be expressed as:

$$SINR_k = \frac{\mathbf{w}_k \mathbf{f}_k \mathbf{f}_k^* \mathbf{TR} \mathbf{TR}^* \mathbf{w}_k^*}{\mathbf{w}_k^* (\mathbf{I}_k \mathbf{I}_k^* \mathbf{f}_i \mathbf{f}_i^*) \mathbf{w}_k^*} \quad (2)$$

179 The achievable capacity for the three underground EM components is defined as:

$$C = \sum_{k=1}^3 \log_2(1 + SINR_k) \quad (3)$$

180 Since the objective of this approach is to enhance the channel gain and to remove the
181 inter-component interference, we have only considered the beamforming vectors under the lower
182 bound of achievable capacity. Therefore, maximum rate is not achieved because only the product
183 achievable rate is utilized. Next we present the approach to completely remove the inter-component
184 interference. The the instantaneous SNR for every sensed component can be defined as follows when
185 the receive beamforming is not employed at [32]:

$$\gamma_i = \frac{E_b |h_i|^2}{N_0}, \quad (4)$$

186 where i represents the L , D , or R components. The E_b is the energy per bit and the $|h_i|$ denotes the
187 impulse response.

188 A three fold increase in SNR (in comparison to a single antenna match filter based design) can be
189 achieved by employing the maximum ratio combining (MRC) approach [32,51]:

$$\gamma = \sum_{i=1}^3 w_i \frac{E_b |h_i|^2}{N_0}, \quad (5)$$

190 where w_i is the weighting factor used for combining. Although SISO approach can be used to maximize
191 the gain, but the reflected components still cause some interference. Therefore, in order to eliminate the
192 undesired interference, the UG MIMO uses transmit beamforming vectors. Accordingly, the received
193 signal can be expressed as [50]:

$$y_k = \mathbf{w}_k^* \mathbf{TR} \mathbf{f}_k x_k + \mathbf{w}_k^* \mathbf{I}_k \mathbf{f}_i x_i + \mathbf{w}_k^* n_k \quad (6)$$

$$y_k = \frac{\mathbf{w}_k^* \mathbf{TR} \mathbf{f}_k x_k}{\|\mathbf{TR} \mathbf{f}_i\|} + \frac{\mathbf{w}_k^* \mathbf{I}_k \mathbf{f}_i x_i}{\|\mathbf{TR} \mathbf{f}_i\|} + \frac{\mathbf{w}_k^* n_k}{\|\mathbf{TR} \mathbf{f}_i\|} \quad (7)$$

194 To completely eliminate the interference from (7), MRC approach should satisfy following:

$$\mathbf{w}_1^* \mathbf{I}_1 \mathbf{f}_i = 0 \quad (8)$$

195 that can be satisfied by using the transmit beamforming vector. Using this zero interference
196 constraint, MRC beamforming vectors are generalized eigenvectors.

197 In addition to environment aware weights of UG MIMO, which are based on soil moisture sensing,
198 feedback signals are used to adjust the weights by using the array gain feedback loops. This problem
199 is formulated as maximizing the array gain by using the pilot signals. In this method, UG MIMO array
200 at the transmitter receives the pilot signal in receive mode and then accordingly adjusts its parameters
201 for the transmit mode. In receive mode at the transmitter, scan angles are varied to get the estimate
202 of channel state. The best SNR statistics are used and with change in soil moisture, parameters are
203 adjusted accordingly.

For an array of identical elements, the far-field power density is expressed as [52]:

$$P_{den} = \frac{|E(\theta, \phi)|^2}{120\pi}, \quad (9)$$

where $E(\theta, \phi)$ is the electric field intensity of the individual array element and is given as:

$$|E(\theta, \phi)| = \sqrt{P_{et}} \sqrt{G_{et}} \frac{\sqrt{30}}{d}, \quad (10)$$

where P_{et} , G_{et} are element transmit power and gain, respectively, and d is the distance. E-field
contributions (E_a) from all elements are added together to calculate the array gain G_a [52]. Therefore,

$$G_a(\theta, \phi) = \frac{d^2 |E_a \zeta(\theta, \phi)|^2}{30 P_t}, \quad (11)$$

where ζ is the element phase factor and

$$E_a = \frac{\sqrt{30}}{d} \sum_n \sqrt{P_{et}} \sqrt{G_{et}}. \quad (12)$$

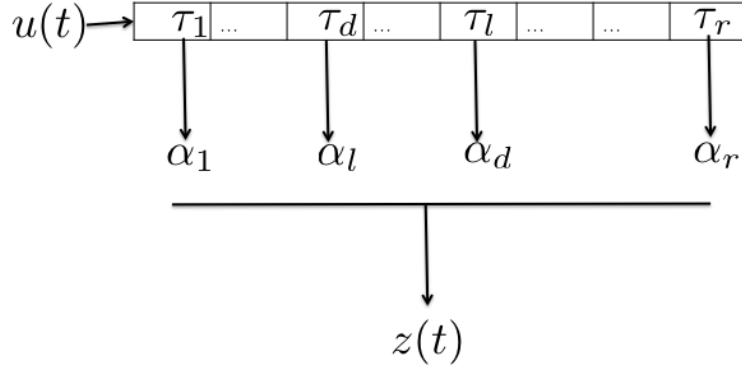


Figure 3. A realization of the UG channel model with three components.

The received power is presented next. Effective isotropic radiated power (EIRP) can be expressed as product of the transmitted power and antenna gain:

$$P_{rad} = G_t P_t, \quad (13)$$

204 where P_t is the transmitted power and G_t is the array gain.

The far-field power density P_{av} can be expressed as [53]:

$$P_{av} = P_{av}^D + P_{av}^R + P_{av}^L. \quad (14)$$

where D, R, L denotes the power densities of the direct, reflected and lateral component [30]. The received power is calculated as the product of far-field power density P_{av} and antenna aperture ($\lambda_s^2/4\pi$). The received power is given as [53]:

$$\begin{aligned} P_r^d &= P_t + 20 \log_{10} \lambda_s - 20 \log_{10} r_1 - 8.69 \alpha_s r_1 \\ &\quad - 22 + 10 \log_{10} D_{rl}, \\ P_r^r &= P_t + 20 \log_{10} \lambda_s - 20 \log_{10} r_2 - 8.69 \alpha_s r_2 \\ &\quad + 20 \log_{10} \Gamma - 22 + 10 \log_{10} D_{rl}, \\ P_r^l &= P_t + 20 \log_{10} \lambda_s - 40 \log_{10} d - 8.69 \alpha_s (h_t + h_r) \\ &\quad + 20 \log_{10} T - 22 + 10 \log_{10} D_{rl}, \end{aligned} \quad (15)$$

where Γ and T are reflection and transmission coefficients [53], and λ_s is the wavelength in soil. The received power, for an isotropic antenna, is expressed as [53]:

$$P_r = 10 \log_{10} (10^{\frac{P_r^d}{10}} + 10^{\frac{P_r^r}{10}} + 10^{\frac{P_r^l}{10}}). \quad (16)$$

205 5. Performance Analysis

206 In this section, we present the performance analysis of the UG MIMO. First, the model evaluations
207 and results of the transmit beamforming are presented in the next section.

208 5.1. Transmit Beamforming

209 To evaluate the developed scheme, we consider the transmit MMSE, ZFBF, and MRT
210 beamforming of [54]. The implementation of the heuristic beamforming schemes (MRT, ZFBF, transmit
211 MMSE/regularized ZFBF/SLNR-MAX beamforming, and the corresponding power allocation) is also

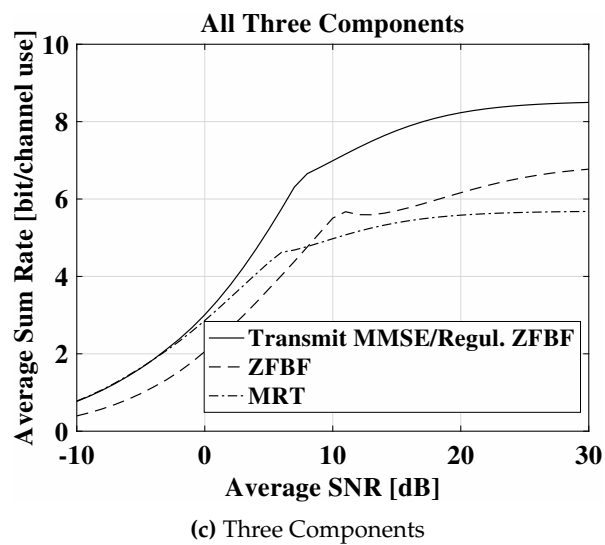
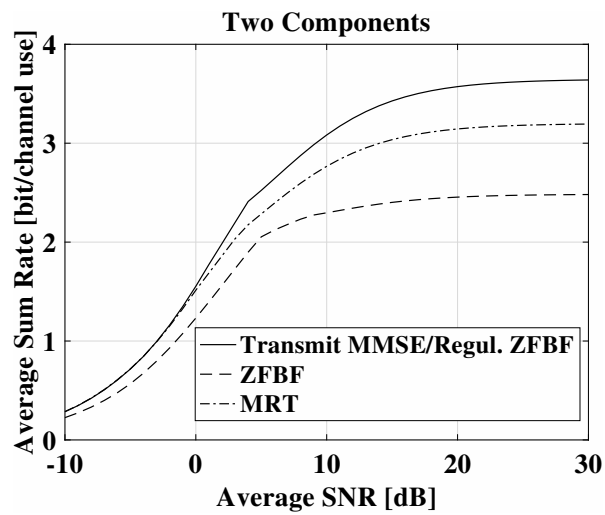
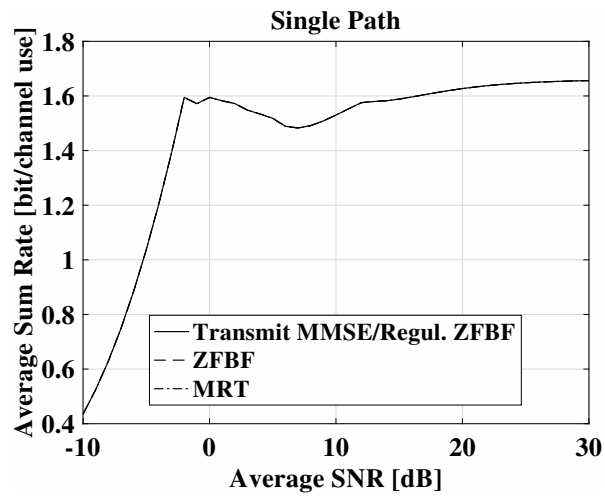


Figure 4. UG MIMO: The average sum rate (bit/channel use) as a function of change in average SNR.

212 based on the [54]. For the UG MIMO application, instead of randomly generating OTA channels, we
 213 use the UG channel impulse response [30], where root mean square (RMS) delay spread, distribution
 214 of the RMS delay spread, mean amplitude across multiple profiles for a fixed T-R displacement,
 215 effects of soil moisture on peak amplitudes of power delay profiles, mean access delay, and coherence
 216 bandwidth statistics are presented based on the measured data collected from UG channel experiments.
 217 A realization of the UG channel model is shown in Fig. 3. It is important to note here that the calculation
 218 of optimal beamforming is not performed in this work because of its computational complexity [55].
 219 The range of the considered SNR values is -10 dB to 30 dB.

220 For the simulations, the beamforming matrices are generated for sum rates with different
 221 beamforming strategies (e.g., MRT, ZFBF, transmit MMSE/regularized ZFBF/SLNR-MAX).
 222 Accordingly, UG MIMO evaluation is done for different paths of the underground channel. The
 223 direct, lateral, and the reflected paths of the underground channel are considered. After the channel
 224 matrices are generated for all realizations, accordingly, for each realization normalized beamforming
 225 matrices are computed for each approach. Furthermore, by using the branch-reduce-and-bound (BRB)
 226 algorithm, based on the proposed approach, pre-allocate matrix serves as the feasible starting points
 227 for the BRB algorithm.

228 Accordingly, the system iterates through all powers. Due to its dependency on the transmit
 229 power, the normalized beamforming vectors for transmit MMSE beamforming (which is the same
 230 as regularized ZFBF and SLNR-MAX beamforming) are also computed similarly. The sum rate is
 231 calculated accordingly for the three different beamforming approaches.

232 Next, we present the evaluations done using these beamforming approaches for the three different
 233 components. In Figs. 4, the average sum rate (bit/channel use) is shown as a function of change in
 234 average SNR. The case in which only the single (direct) element is considered is shown in Fig. 4(a). It
 235 can be observed that the average sum rate range is 1.5 to 1.7 and it does not change significantly with
 236 change in average SNR. Because, in the case of single component, there is no beamforming involved.
 237 Therefore, all three approaches have the same average sum rate.

238 In Fig. 4(b), the average sum rate for the direct and reflected components (two component case)
 239 is shown. In comparison to the single path scenario, it can be observed that average sum rate has
 240 increased from 1.6 to 3.1 at the average SNR value of 10 dB. Moreover, for the two component case,
 241 it can also be observed that the at the lower average SNR of 0 dB, there is only minor difference of
 242 0.1 average sum rate between the three beamforming approaches. At the average SNR of 10 dB, the
 243 difference between ZFBF and MMSE is increased to 0.7 , which shows that the UG MIMO approach
 244 has the better performance as compared to the ZFBF. This difference further increases with increase in
 245 SNR which shows that in higher SNR regimes, the UG MIMO transmission approach leads to even
 246 improved performance gain.

247 This better performance of the UG MIMO transmit beamforming improves further in the three
 248 component scenario where all three components (e.g., direct, lateral, and reflected) are used transmit
 249 beamforming. This scenario has been shown in Fig. 4(c). Overall, the three components beamforming
 250 scenario leads to significant performance improvements as compared to the two path transmit
 251 beamforming case. In comparison to the two path scenario, it can be observed that average sum
 252 rate has increased from 3.1 to 6.6 at the average SNR value of 10 dB. Moreover, for the three component
 253 case, it can also be observed that even the at the lower average SNR of 0 dB, there are minor difference
 254 of average sum rate between the three beamforming approaches. At the average SNR of 10 dB, the
 255 difference between ZFBF and MMSE is increased to 2.7 . It is also interesting to note that at the
 256 average SNR of 30 dB, the average sum rate reached at the maximum value of 8.4 which shows that the
 257 UG MIMO approach performs best when all three components are used for underground transmit
 258 beamforming.

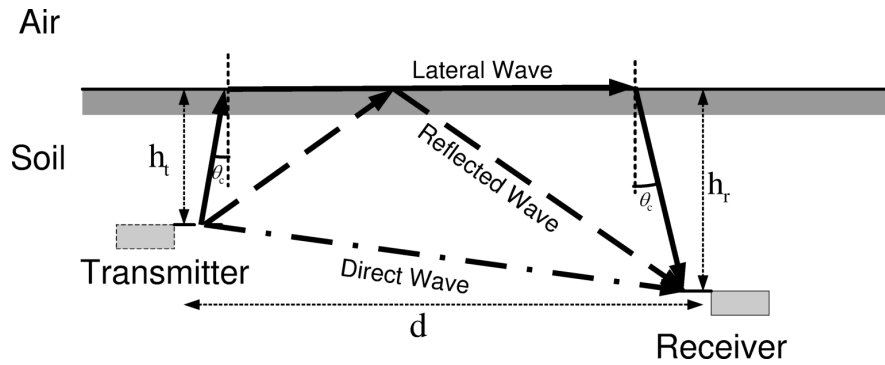


Figure 5. The direct, reflected, and lateral waves in the underground channel [30].

259 5.2. Receive Beamforming

260 For the receive beamforming of the UG MIMO, a 16-element uniform linear array with
 261 inter-element distance of half wavelength is used. The operation frequency of 300 MHz is employed.
 262 In underground communications, a higher path loss is observed at higher frequencies [30]. The
 263 soil has higher permittivity as compared to the air, which leads to the wavelength shortening. Due
 264 to the soil permittivity factor, frequency bands in lower spectrum are more suitable for long range
 265 communications. Moreover, distance, depth, and soil water content also affects the path loss in
 266 underground communications, which requires environment-aware operation frequency selection.

267 We consider the reception of the received signal through the UG MIMO receive beamforming. In
 268 UG communications, there are three main components (e.g. direct, lateral, and reflected (see Fig. 5)).
 269 The received signal that originates from 10-15° azimuth has the highest received power. The UG
 270 channel has excess delays extending up to 100 ns and root mean square (RMS) delay spread values up
 271 to 50 ns. The attenuation varies over 50 dB dynamic range. The direct wave (second received signal) is
 272 received from 90° azimuth (direct path, line-of-sight component). It is also known that arrival time of
 273 multipath components follows lateral wave based 3-wave UG channel model such that the direct wave
 274 reaches at the receiver first before the lateral and reflected components for shorter communication
 275 distances [30]. The third wave (the reflected signal) travels towards to the soil-air interface and reaches
 276 at the receiver from 45° azimuth. Its total path is also completely through the soil.

277 The three received signals at the UG MIMO receiver are not correlated with each other and can
 278 be distinguished because of different propagation speed in the stratified soil medium. This leads to
 279 different inter-element delays that assist different these elements in time. The uniform white noise is
 280 considered across all array elements. A beam-scan spatial spectrum estimator is used based on the
 281 arrival directions of these three components of the underground channel impulse response.

282 In Fig. 6, the spatial spectrum of the three components in the UG MIMO receive beamforming
 283 is shown. The plot shows a high power gains at 10° which corresponds to the lateral wave. The
 284 lower power gain is exhibited at the 90°, which represents the direct wave. The lower peak at the 45°
 285 indicates the reflected wave that due to the lower path in the soil has the lowest gain.

286 6. Air-Soil Interface Impact Adjustment

287 In this section, we discuss the air-soil interface impact adjustment mechanism of the subsurface
 288 MIMO, which constitutes as the new contribution of this paper as compared with the preliminary
 289 conference version [1]. When subsurface beam is directed in isotropic directions particularly to the
 290 air-soil interface, the refraction mechanism leads to beam disorientation when incident at the soil-air
 291 interface. The soil-air interface separates the soil medium form air and both have different properties
 292 which give rise to refraction of waves. This phenomena is also called the beam squint [56]. The
 293 resulting error because of beam squint can range from 5 to 15 deg depending on the the amount soil
 294 water content present in the medium. It also depends on the incidence angle at the air-soil interface.

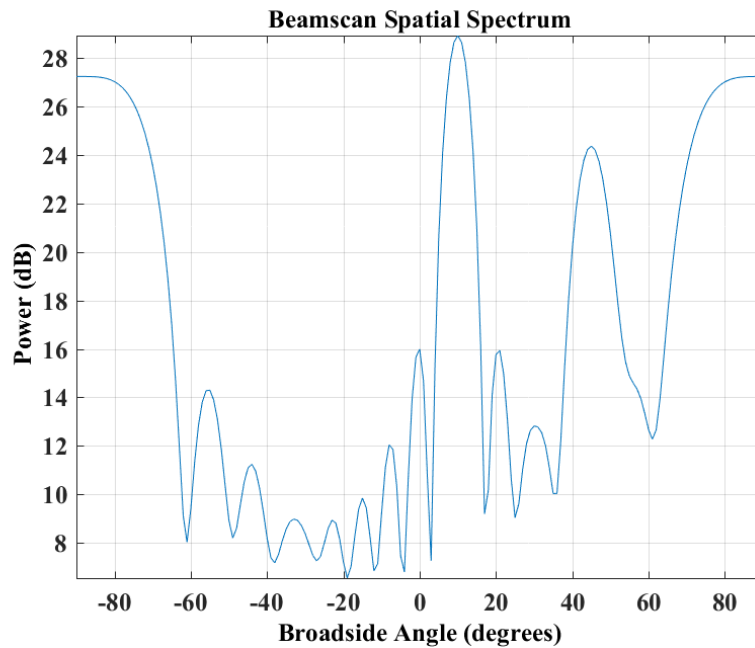


Figure 6. The spatial spectrum of the three components of the UG MIMO receive beamforming.

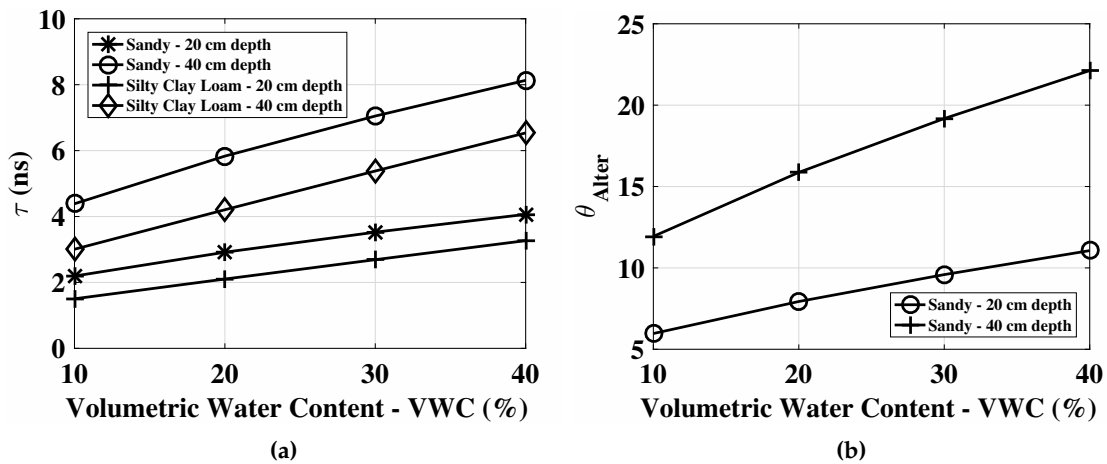


Figure 7. (a) τ with 10%-40% change in soil moisture in sandy and silty clay loam soils at 20 cm and 40 cm depth. (b) Corresponding phase shift adjustment to original phase in sandy soil for 10%-40% change in soil moisture at 20 cm and 40 cm depth.

295 The refraction also impacts the wave propagation velocity both in the soil and air medium. This effect
 296 can be corrected by using the time delays (τ) and optimum angle adjustment.

297 In Fig. 7(a), τ is shown for 10%-40% change in soil moisture values in sandy and silty clay loam
 298 soils at 20 cm and 40 cm depth. It can be observed that higher soil moisture levels lead to increase in
 299 delay and it further increases by increasing the depth. The corresponding phase shift adjustment to
 300 original phase in sandy soil for 10%-40% change in soil moisture at 20 cm and 40 cm depth is shown in
 301 Fig.7(a). Therefore, larger adjustments are required for higher soil moisture levels and higher depths.

302 6.1. Array Optimization

303 In the UG settings, wavelength variations not only effect the directivity and but also cause grating
 304 lobes, which cause beam patterns to appear in undesired directions. We analyze this effect in the

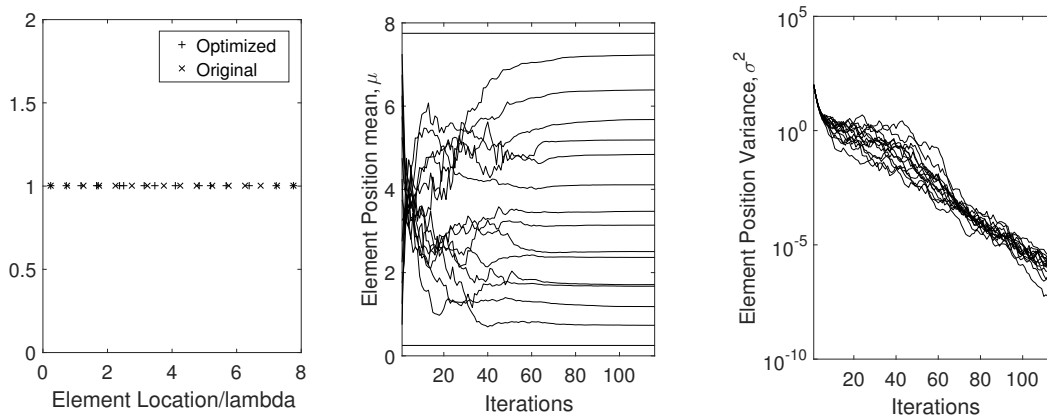


Figure 8. The array optimization results.

305 UG communications. This problem can be solved by either frequency-agile operation to keep the
 306 wavelength fixed by using tuning, or by selecting the elements to mitigate the effects of wave length
 307 changes.

308 By using genetic algorithm [56], that work on the natural selection process. Overall, this results
 309 in complete optimization of array, which is robust to mechanisms taking place in the soil. By using
 310 this technique, an initial inter-element position can either be specified or chosen arbitrarily. A priori
 311 position is based on the actual position without consideration of the particular soil moisture level. Cost
 312 (score) function of is evaluated and desired inter-element spacing is determined. Element position
 313 optimization results are shown in Fig. 8.

314 7. Conclusions and Future Work

315 Underground wireless communications in the soil medium is challenging due to the impacts of
 316 soil texture and soil water content. In subsurface radio wave propagation, the phased array antennas
 317 can be utilized to direct the wave power by using the Zenneck waves which leads to underground
 318 communication range extension and energy conservation. In this paper, a design of subsurface phased
 319 array antennas for digital agriculture applications has been presented. An UG MIMO technique is
 320 developed for transmit and receive beamforming in the underground soil medium. The optimal
 321 transmit beamforming and receive combining vectors under minimal inter-component interference
 322 constraint are derived. It is shown that UG MIMO performs best when all three component of the
 323 wireless UG channel are leveraged for beamforming. The environment aware UG MIMO technique
 324 leads to three-fold performance improvements and paves the wave for design and development of
 325 next generation sensor-guided irrigation systems in the field of digital agriculture.

326 The transmit beamforming is used to focus energy in the desired direction, there are three different
 327 paths in the underground soil medium through which the waves propagates to reach at the receiver.
 328 When the UG receiver receives a desired data stream only from the desired path, then the UG MIMO
 329 channel becomes three path (lateral, direct, and reflected) interference channel. Accordingly, the
 330 capacity region of the UG MIMO three path interference channel and degrees of freedom (multiplexing
 331 gain of this MIMO channel requires careful modeling. Therefore, expressions are required for the
 332 degree of freedom of the UG MIMO interference channel. The underground receiver needs to perfectly
 333 cancel the interference from the three different components of the EM-waves propagating in the soil
 334 medium. This concept is based upon reducing the interference the undesired components to minimum
 335 at UG receiver using the receive beamforming. Accordingly, an underground environment aware

336 MIMO using transmit and receive beamforming is developed. Moreover, environment aware UG
337 MIMO techniques are designed and investigated in the underground soil medium.

338 Any implementation of subsurface phased array is likely to be complicated and expensive as
339 compared to existing solutions. Moreover, practical implementation of subsurface phased array
340 integrated with soil moisture sensing, and optimization is a challenging task. For future work,
341 the decreasing cost and complexity of hardware, and utilizing the long range, high data rate UG
342 communications, compared to conventional solutions, makes subsurface phased array a viable
343 candidate for the next generation wireless UG communication systems.

344 **Conflicts of Interest:** The authors declare no conflict of interest.

345

- 346 1. Salam, A. Underground Environment Aware MIMO Design Using Transmit and Receive Beamforming in
347 Internet of Underground Things. 2019 International Conference on Internet of Things (ICIOT 2019); , 2019.
- 348 2. Salam, A. Pulses in the Sand: Long Range and High Data Rate Communication Techniques for next
349 Generation Wireless Underground Networks. *ETD collection for University of Nebraska - Lincoln* **2018**.
- 350 3. Salam, A.; Vuran, M.C. EM-Based Wireless Underground Sensor Networks. In
351 *Underground Sensing*; Pamukcu, S.; Cheng, L., Eds.; Academic Press, 2018; pp. 247 – 285.
352 doi:<https://doi.org/10.1016/B978-0-12-803139-1.00005-9>.
- 353 4. Salam, A.; Vuran, M.C.; Irmak, S. Di-Sense: In situ real-time permittivity estimation and soil
354 moisture sensing using wireless underground communications. *Computer Networks* **2019**, *151*, 31 – 41.
355 doi:<https://doi.org/10.1016/j.comnet.2019.01.001>.
- 356 5. Abrudan, T.E.; Kypris, O.; Trigoni, N.; Markham, A. Impact of Rocks and Minerals on
357 Underground Magneto-Inductive Communication and Localization. *IEEE Access* **2016**, *4*, 3999–4010.
358 doi:10.1109/ACCESS.2016.2597641.
- 359 6. Akyildiz, I.F.; Stuntebeck, E.P. Wireless Underground Sensor Networks: Research Challenges. *Ad Hoc*
360 *Networks Journal* **2006**.
- 361 7. Bogena, H.R.; Herbst, M.; Huisman, J.A.; Rosenbaum, U.; Weuthen, A.; Vereecken, H. Potential of wireless
362 sensor networks for measuring soil water content variability. *Vadose Zone Journal* **2010**.
- 363 8. Dong, X.; Vuran, M.C.; Irmak, S. Autonomous precision agriculture through integration of wireless
364 underground sensor networks with center pivot irrigation systems. *Ad Hoc Networks* **2013**, *11*, 1975–1987.
- 365 9. Guo, H.; Sun, Z. Channel and Energy Modeling for Self-Contained Wireless Sensor Networks in Oil
366 Reservoirs. *IEEE Trans. Wireless Communications* **2014**, *13*, 2258–2269. doi:10.1109/TWC.2013.031314.130835.
- 367 10. Konda, A.; Rau, A.; Stoller, M.A.; Taylor, J.M.; Salam, A.; Pribil, G.A.; Argyropoulos, C.; Morin, S.A. Soft
368 Microreactors for the Deposition of Conductive Metallic Traces on Planar, Embossed, and Curved Surfaces.
369 *Advanced Functional Materials*, *28*, 1803020. doi:10.1002/adfm.201803020.
- 370 11. Markham, A.; Trigoni, N. Magneto-inductive Networked Rescue System (MINERS): Taking Sensor
371 Networks Underground. Proceedings of the 11th ICPS. ACM, 2012, IPSN '12, pp. 317–328.
372 doi:10.1145/2185677.2185746.
- 373 12. Salam, A.; Vuran, M.C. Impacts of Soil Type and Moisture on the Capacity of Multi-Carrier Modulation in
374 Internet of Underground Things. Proc. ICCCN 2016; , 2016.
- 375 13. Salam, A.; Vuran, M.C.; Irmak, S. Towards Internet of Underground Things in Smart Lighting: A Statistical
376 Model of Wireless Underground Channel. Proc. 14th IEEE International Conference on Networking,
377 Sensing and Control (IEEE ICNSC); , 2017.
- 378 14. Salam, A.; Shah, S. Internet of Things in Smart Agriculture: Enabling Technologies. 2019 IEEE 5th World
379 Forum on Internet of Things (WF-IoT) (WF-IoT 2019); , 2019.
- 380 15. Salam, A. Underground Soil Sensing Using Subsurface Radio Wave Propagation. 5th Global Workshop on
381 Proximal Soil Sensing; , 2019.
- 382 16. Salam, A.; Shah, S. Urban Underground Infrastructure Monitoring IoT: The Path Loss Analysis. 2019 IEEE
383 5th World Forum on Internet of Things (WF-IoT) (WF-IoT 2019); , 2019.

- 384 17. Salam, A.; Vuran, M.C.; Dong, X.; Argyropoulos, C.; Irmak, S. A Theoretical Model of Underground Dipole
385 Antennas for Communications in Internet of Underground Things. *IEEE Transactions on Antennas and*
386 *Propagation* **2019**.
- 387 18. Salam, A. A Comparison of Path Loss Variations in Soil using Planar and Dipole Antennas. 2019 IEEE
388 International Symposium on Antennas and Propagation. IEEE, 2019.
- 389 19. Salam, A. A Path Loss Model for Through the Soil Wireless Communications in Digital Agriculture. 2019
390 IEEE International Symposium on Antennas and Propagation. IEEE, 2019.
- 391 20. Salam, A. An Underground Radio Wave Propagation Prediction Model for Digital Agriculture. *Information*
392 **2019**, *10*. doi:10.3390/info10040147.
- 393 21. Tiisanen, M.J. Soil Scouts: Description and performance of single hop wireless underground sensor nodes.
394 *Ad Hoc Networks* **2013**, *11*, 1610 – 1618. doi:http://dx.doi.org/10.1016/j.adhoc.2013.02.002.
- 395 22. Vuran, M.C.; Salam, A.; Wong, R.; Irmak, S. Internet of underground things in precision
396 agriculture: Architecture and technology aspects. *Ad Hoc Networks* **2018**, *81*, 160 – 173.
397 doi:https://doi.org/10.1016/j.adhoc.2018.07.017.
- 398 23. Vuran, M.C.; Salam, A.; Wong, R.; Irmak, S. Internet of Underground Things: Sensing and Communications
399 on the Field for Precision Agriculture. 2018 IEEE 4th World Forum on Internet of Things (WF-IoT) (WF-IoT
400 2018); , 2018.
- 401 24. Akyildiz, I.F.; Sun, Z.; Vuran, M.C. Signal Propagation Techniques for Wireless Underground
402 Communication Networks. *Physical Communication Journal (Elsevier)* **2009**, *2*, 167–183.
- 403 25. Sun, Z.; Wang, P.; Vuran, M.C.; Al-Rodhaan, M.A.; Al-Dhelaan, A.M.; Akyildiz, I.F. Border patrol through
404 advanced wireless sensor networks. *Ad Hoc Networks* **2011**, *9*, 468–477.
- 405 26. Temel, S.; Vuran, M.C.; Lunar, M.M.; Zhao, Z.; Salam, A.; Faller, R.K.; Stolle, C. Vehicle-to-barrier
406 communication during real-world vehicle crash tests. *Computer Communications* **2018**, *127*, 172 – 186.
407 doi:https://doi.org/10.1016/j.comcom.2018.05.009.
- 408 27. Sun, Z.; Akyildiz, I. Channel modeling and analysis for wireless networks in underground mines and road
409 tunnels. *IEEE Trans. on Communications* **2010**. doi:10.1109/TCOMM.2010.06.080353.
- 410 28. Sun, Z.; et.al.. MISE-PIPE: MI based wireless sensor networks for underground pipeline monitoring. *Ad*
411 *Hoc Networks* **2011**.
- 412 29. Salam, A.; Vuran, M.C. Smart Underground Antenna Arrays: A Soil Moisture Adaptive Beamforming
413 Approach. Proc. IEEE INFOCOM 2017; , 2017.
- 414 30. Salam, A.; Vuran, M.C.; Irmak, S. Pulses in the Sand: Impulse Response Analysis of Wireless Underground
415 Channel. Proc. IEEE INFOCOM 2016;
- 416 31. Salam, A.; Karabiyik, U. A Cooperative Overlay Approach at the Physical Layer of Cognitive Radio for
417 Digital Agriculture. Third International Balkan Conference on Communications and Networking 2019
418 (BalkanCom'19); , 2019.
- 419 32. Salam, A.; Vuran, M.C. Wireless Underground Channel Diversity Reception with Multiple Antennas for
420 Internet of Underground Things. Proc. IEEE ICC 2017; , 2017.
- 421 33. Baranwal, T.; Pateriya, P.K.; others. Development of IoT based smart security and monitoring devices
422 for agriculture. 2016 6th International Conference-Cloud System and Big Data Engineering (Confluence).
423 IEEE, 2016, pp. 597–602.
- 424 34. Kisseleff, S.; Akyildiz, I.F.; Gerstacker, W.H. Survey on Advances in Magnetic Induction-Based
425 Wireless Underground Sensor Networks. *IEEE Internet of Things Journal* **2018**, *5*, 4843–4856.
426 doi:10.1109/JIOT.2018.2870289.
- 427 35. Suciu, G.; Istrate, C.; Dițu, M. Secure smart agriculture monitoring technique through isolation. 2019
428 Global IoT Summit (GIoTS), 2019, pp. 1–5. doi:10.1109/GIOTS.2019.8766433.
- 429 36. Borgia, E. The Internet of Things vision: Key features, applications and open issues. *Computer*
430 *Communications* **2014**, *54*, 1 – 31. doi:https://doi.org/10.1016/j.comcom.2014.09.008.
- 431 37. Tzounis, A.; Katsoulas, N.; Bartzanas, T.; Kittas, C. Internet of Things in agriculture, recent advances and
432 future challenges. *Biosystems Engineering* **2017**, *164*, 31–48.
- 433 38. Liu, X.; et.al.. DIRC: Increasing Indoor Wireless Capacity Using Directional Antennas. *SIGCOMM Comput.*
434 *Commun. Rev.* **2009**.

- 435 39. Lakshmanan, S.; Sundaresan, K.; Kokku, R.; Khojastepour, A.; Rangarajan, S. Towards Adaptive
436 Beamforming in Indoor Wireless Networks: An Experimental Approach. *INFOCOM 2009, IEEE*, 2009.
437 doi:10.1109/INFOCOM.2009.5062199.
- 438 40. Kontaxis, D.; et.al.. Optimality of Transmit Beamforming in Spatially Correlated MIMO Rician Fading
439 Channels. *Wir. Per. Comm.* **2016**.
- 440 41. Quitin, F.; et.al.. A Scalable Architecture for Distributed Transmit Beamforming with Commodity
441 Radios: Design and Proof of Concept. *IEEE Trans. on Wireless Communications* **2013**.
442 doi:10.1109/TWC.2013.012513.121029.
- 443 42. Nitsche, T.; et.al.. Steering with eyes closed: Mm-Wave beam steering without in-band measurement. *IEEE*
444 *INFOCOM*, 2015. doi:10.1109/INFOCOM.2015.7218630.
- 445 43. Anand, N.; Lee, S.J.; Knightly, E.W. STROBE: Actively securing wireless communications
446 using Zero-Forcing Beamforming. *INFOCOM, 2012 Proceedings IEEE*, 2012, pp. 720–728.
447 doi:10.1109/INFOCOM.2012.6195817.
- 448 44. Aryafar, E.; et.al.. ADAM: An Adaptive Beamforming System for Multicasting in Wireless LANs.
449 *IEEE/ACM Trans. on Networking* **2013**. doi:10.1109/TNET.2012.2228501.
- 450 45. Widrow, B.; et.al.. Adaptive antenna systems. *Proceedings of the IEEE* **1967**. doi:10.1109/PROC.1967.6092.
- 451 46. Alexandropoulos, G.C.; Ferrand, P.; m. Gorce, J.; Papadias, C.B. Advanced coordinated
452 beamforming for the downlink of future LTE cellular networks. *IEEE Communications Magazine* **2016**.
453 doi:10.1109/MCOM.2016.7509379.
- 454 47. Du, Y.; et.al.. iBeam: Intelligent client-side multi-user beamforming in wireless networks. *IEEE INFOCOM*
455 *2014, 2014*. doi:10.1109/INFOCOM.2014.6848009.
- 456 48. Kisseleff, S.; Akyildiz, I.F.; Gerstacker, W. Beamforming for Magnetic Induction Based
457 Wireless Power Transfer Systems with Multiple Receivers. *2015 IEEE GLOBECOM*, 2015.
458 doi:10.1109/GLOCOM.2015.7417006.
- 459 49. King, R.W.P.; Smith, G. *Antennas in Matter*; MIT Press, 1981.
- 460 50. Chae, C.B.; Hwang, I.; Heath, R.W.; Tarokh, V. Interference Aware-Coordinated Beamforming
461 in a Multi-Cell System. *IEEE Transactions on Wireless Communications* **2012**, *11*, 3692–3703.
462 doi:10.1109/TWC.2012.081312.112119.
- 463 51. Proakis, J.; Salehi, M. *Digital Communications*, 5th ed.; McGraw-Hill, 2007.
- 464 52. Fenn, A.; Hurst, P. *Ultrawideband Phased Array Antenna Technology for Sensing and Communications Systems*;
465 MIT Press, 2015.
- 466 53. Dong, X.; Vuran, M.C. A Channel Model for Wireless Underground Sensor Networks Using Lateral Waves.
467 *Proc. of IEEE Globecom '11*; , 2011.
- 468 54. Bjornson, E.; Bengtsson, M.; Ottersten, B. Optimal multiuser transmit beamforming: A difficult problem
469 with a simple solution structure. *IEEE Signal Processing Magazine* **2014**, *31*, 142–148.
- 470 55. Björnson, E.; Bengtsson, M.; Ottersten, B. Optimal multiuser transmit beamforming: A difficult problem
471 with a simple solution structure [lecture notes]. *IEEE Signal Processing Magazine* **2014**, *31*, 142–148.
- 472 56. Haupt, R. *Timed Arrays*; Wiley, 2015.